



# Influence of Chemical Kinetics on Predictions of Performance of Syngas Production From Fuel-Rich Combustion of CO<sub>2</sub>/CH<sub>4</sub> Mixture in a Two-Layer Burner

Junrui Shi<sup>1</sup>, Mingming Mao<sup>1\*</sup>, Houping Li<sup>1</sup>, Yongqi Liu<sup>1</sup>, Yang Liu<sup>2</sup> and Yangbo Deng<sup>2</sup>

<sup>1</sup> School of Transportation and Vehicle Engineering, Shandong University of Technology, Zibo, China, <sup>2</sup> Marine Engineering College, Dalian Maritime University, Dalian, China

## OPEN ACCESS

### Edited by:

Davide Fissore,  
Politecnico di Torino, Italy

### Reviewed by:

Alexei V. Saveliev,  
North Carolina State University,  
United States  
Aiwu Fan,  
Huazhong University of Science and  
Technology, China

### \*Correspondence:

Mingming Mao  
shandongmao@163.com

### Specialty section:

This article was submitted to  
Chemical and Process Engineering,  
a section of the journal  
Frontiers in Chemistry

Received: 20 May 2019

Accepted: 13 December 2019

Published: 21 January 2020

### Citation:

Shi J, Mao M, Li H, Liu Y, Liu Y and  
Deng Y (2020) Influence of Chemical  
Kinetics on Predictions of  
Performance of Syngas Production  
From Fuel-Rich Combustion of  
CO<sub>2</sub>/CH<sub>4</sub> Mixture in a Two-Layer  
Burner. *Front. Chem.* 7:902.  
doi: 10.3389/fchem.2019.00902

Numerical investigations on partial oxidation combustion of CO<sub>2</sub>/CH<sub>4</sub> mixture were executed for a two-layer burner using a two-dimensional two-temperature model with different detailed chemical reaction mechanisms that are DRM 19, GRI-Mech 1.2, and GRI-Mech 3.0. Attention was focused on the influence of these mechanisms on predictions of the temperature distributions in the burner, chemical structure as well as syngas production. The equivalence ratio was a fixed value of 1.5, while the volumetric ratio of CO<sub>2</sub> to CH<sub>4</sub> was changed from 0 to 1. The predicted results were compared with the available experimental data. It was revealed that the chemical reaction mechanisms have little effect on the temperature distribution in the burner except for the exothermic zone. It indicated that the smaller kinetic DRM 19 can precisely predict the temperature distributions in the burner, using DRM 19 was recommended to save computational time when the detailed components of the syngas was not taken into consideration. In addition, all the three mechanisms predicted the same trend of molar fraction of CO, H<sub>2</sub>, and CO<sub>2</sub> with experimental results. Good agreement between the experiment and predictions of major species was obtained by GRI-Mech 1.2 and GRI-Mech 3.0, the two mechanisms had the same accuracy in predicting CO, H<sub>2</sub>, and CO<sub>2</sub> production. However, computations with DRM 19 under-predicted the molar fraction of CO and H<sub>2</sub>. Furthermore, it was shown that the thermal conductivity of porous media has significant effect on the syngas production. In general, the temperature was increased as the thermal conductivity of the porous media was reduced and the H<sub>2</sub> production was increased.

**Keywords:** fuel-rich combustion, porous media, syngas production, numerical study, chemical kinetics

## HIGHLIGHTS

- The highest combustion temperature in the reaction zone is predicted by DRM 19
- Computations by DRM 19 under-predict the molar fraction of CO and H<sub>2</sub>
- GRI-Mech 3.0 and 1.2 have the same accuracy in predicting the syngas component;
- Increase in thermal conductivity of solid leads to increase in temperature in the two-layer burner;
- Increase in thermal conductivity of solid leads to increase in H<sub>2</sub> production.

## INTRODUCTION

The interest in syngas production from fuel-rich partial oxidation within inert porous media has increased significantly during the last two decades. This is because this technology combines several positive features, such as quick start-up, fast dynamic response, no need for external heat, steam, and catalyst. Kennedy et al. (1999) and Muhammad (2016) presented detailed reviews of this subject.

In order to improve combustion process and increase syngas production, a large amount of researches have been conducted in recent years and some significant developments have been made (Mujeebu, 2016).

There are many experimental and numerical studies on fuel-rich partial oxidation in porous media burner. In general, there are two design approaches commonly employed for syngas production in porous burner: the transient combustions systems and stationary systems.

For the transient combustion system, the porous media burner was filled with homogeneous porous media and flame propagations were observed either in downstream or upstream direction in most cases. Hydrogen production by transient filtration combustion was extensively studied by Kennedy group (Drayton et al., 1998), they proposed reciprocal flow burner (RFB) for syngas production and the combustion wave was restricted in the burner by periodically changing the direction of the flow. An extremely high flammability limit was extended to an equivalence ratio of eight for CH<sub>4</sub>/Air mixtures. In the experimental and numerical studies of Kennedy et al. (2000), upstream, downstream, or standing wave was observed experimentally, mainly depending on the CH<sub>4</sub>/Air equivalence ratio ( $\varphi$ ) for the wide range of  $0.2 \leq \varphi \leq 2.5$  and the fixed gas velocity of is 0.25 m/s. The experimental results showed that 60% of the methane was converted to CO and H<sub>2</sub> for  $\varphi > 2$ .

Toledo et al. (2009) studied experimentally the transient combustion system for syngas production in a packed bed filled with 5.6 mm Al<sub>2</sub>O<sub>3</sub> spheres. It was shown that the maximum hydrogen yield was close to 50% and CO yield was close to 80%. To increase the syngas production, two methods were conducted, namely, adding steam during filtration combustion (Araya et al., 2014), or providing external heat source to the burner system (Zheng et al., 2012a). Experimental and numerical results by Araya et al. (2014) showed that hydrogen yield increases with increasing steam content in methane-air mixture. Several fuels conversion to syngas were experimentally studied by Toledo et al. (2016) and Gonzalez et al. (2018), they (Toledo et al., 2016) studied conversion efficiency of partial oxidation combustion in pellet packed bed for liquefied Petroleum Gas, butane, propane, Diesel fuel, and Heavy Fuel Oil. It was shown that conversion efficiency of Heavy Fuel Oil was highest than other fuels and reached up to 45%.

For the transient combustion system, combustion wave always propagates upstream or downstream and this leads to flame extinction at the end. To stabilize the flame within porous burner, two types of burner, namely, RFB (Drayton et al., 1998) and two-layer burner (Zeng et al., 2017; Wang et al., 2018)

filled with different material or structures of the porous media were developed.

For the stationary systems, the burner was filled with different material or structures of porous media, the flame was restricted near two sections of the burners under a certain range of equivalence ratio and gas velocity. Zeng et al. (2017) studied experimentally and numerically the syngas production in a two-layer burner for fuel-rich combustion with a range of CO<sub>2</sub> content in the CH<sub>4</sub> fuel. The experimental results showed that the reforming efficiency increased from 39.1 to 45.3% when the CO<sub>2</sub> was injected into the system. In their subsequent study (Wang et al., 2018), the performance of methane partial oxidation in a two-layer burner filled with alumina pellets of different diameters in the downstream was conducted. According to the highest reforming efficiency, an optimized burner was determined, which was composed of 7.5 mm pellets in the downstream section and 2–3 mm pellets in the upstream section.

For simulation of syngas production from fuel-rich partial oxidation in porous media, it is essential to use detailed or reduced chemistry for investigation of detailed composition of syngas and intermediary components, GRI-Mech combustion mechanism was widely used, which includes detailed Kinetics GRI-Mech 1.2, GRI-Mech 2.11, and GRI-Mech 3.0 (Bowman et al., 2009). For saving computational cost, smaller chemical kinetics like Peters (Mauss and Peters, 1993) or overall mechanism was used by the researchers. Based on the volume-averaged method, one-dimensional or two-dimensional model with these chemical kinetics has been applied to predict the temperature profiles, syngas production, and conversion efficiency.

Kinetic simulations with GRI-Mech 1.2 were conducted and CHEMKIN software was used to solve the chemical reactions (Drayton et al., 1998). Their results indicated that the partial oxidation of methane in porous media occurs ignition and steam reformation processes. Kennedy et al. (2000) analyzed chemical structures of CH<sub>4</sub>/Air mixture in packed bed using one-dimensional model with GRI-Mech 1.2. Their analysis of the reaction pathway showed significant changes of the combustion mechanism from ultra-lean to ultra-rich conditions.

Dhamrat and Ellzey (2006) modeled transient filtration combustion of fuel-rich combustion in the range of equivalence ratio from 1.5 to 5 using a two-dimensional two-temperature model with GRI-Mech 3.0. Special attention was focused on the transient behavior of fuel-rich combustion. It was shown that high solid temperature zone enlarged as combustion wave propagated downstream, which was preferred to steam-reforming reaction and methane conversion efficiency was increased. In addition, they presented the effect of solid properties on the syngas production.

Toledo et al. (2009) modeled syngas production for multiple fuels in porous burner using a one-dimensional two-temperature model with GRI-Mech 3.0. Their predictions showed that fuel-rich partial oxidation in porous media could be used to reform C1-C3 gaseous fuels into hydrogen and syngas. Partial oxidation of methane in a porous reactor was investigated numerically by Zheng et al. (2012a) based on a two-dimensional two-temperature transient model with GRI-Mech 1.2. Results showed

that both the gas and solid temperatures increased in the first 400 s and then the variation of maximum combustion temperature was negligible. To increase the CO and H<sub>2</sub> yields, adding external heat energy for the combustion system was proposed by Zheng et al. (2012b), they modeled partial oxidation of methane in a RFB applying a one-dimensional two-temperature model with GRI-Mech 1.2. Results showed that CO and H<sub>2</sub> yields increased significantly with the external heater power. An industrial reformer was numerically studied using two-dimensional model with GRI-Mech 3.0 and turbulent effect was taken into account (Xu et al., 2014). Their results showed that the methane conversion efficiency increased as the operating pressure was increased and 3.0 MPa was recommended for industrial operation.

Kostenko et al. (2014) modeled methane partial oxidation in a porous reactor using a one-dimensional two-temperature model with detailed kinetic mechanism including soot formation. Their predictions showed that the steam-soot reaction reduces soot formation and increases hydrogen production. An overall three-step six-component chemical kinetic model was developed for methane partial oxidation in porous media (Dobrego et al., 2008). The parameters of kinetic model were derived by adjusting to the experimental conditions and they suggested that the developed model could be combined with detailed chemistry.

To increase conversion efficiency, Dorofeenko and Polianczyk (2016) proposed a new version of RFB for syngas production, in which the methane-steam and air were supplied separately to the RFB. The air was directly feed into the RFB without preheating, whereas the methane-steam was preheated to high temperature prior to entering into the reaction zone by periodically changing the direction of its flow. Zeng et al. (2017) modeled fuel-rich partial oxidation of CH<sub>4</sub>/CO<sub>2</sub> mixture in a two-layer burner using a two-dimensional two-temperature model with the detailed chemical kinetic (Peters). It was shown that the predictions of temperatures and major species matched well with the experimental results. Fuel-rich combustion in porous media was studied using skeleton diagrams and sensitivity analysis (Futko, 2003). They suggested that the combustion wave could be divided into three regions that are preheating zone, exothermic zone and endothermic zone, depending on the heat release.

To save computation time, for fuel-lean combustion in porous media, one-step kinetic still plays an important role in understanding the combustion and heat transfer processes using volume-averaged method (Liu et al., 2009; Fan et al., 2017, 2019; Wang et al., 2019). The influence of chemical reaction mechanisms on predictions of the filtration combustion has been conducted for fuel-lean condition (Hsu and Matthews, 1993; Mohammadi and Hossainpour, 2013). Hsu and Matthews (1993) numerically investigated the effect of chemical reaction mechanisms on the CH<sub>4</sub>/air premixed combustion characteristics in porous media under the condition of equivalence ratio <1. They concluded that it is essential to use multistep kinetics for accurate predictions of temperature profiles, species distribution, energy release rate and pollutant emissions. Mohammadi and Hossainpour (2013) simulated the experiment of Trimis and Durst (1996) applying a two-dimensional two-phase model with different four multistep

kinetics that are GRI-Mech 3.0 mechanism, GRI-Mech 2.11 mechanism, the skeletal and 17 species mechanism (Peters). They studied the effects of these models on temperature, species profiles and pollutant emissions at the fixed equivalence ratio of 0.67 for CH<sub>4</sub>/Air mixture. Results showed that the four models have the same accuracy in predicting temperature distributions and the difference between these profiles was not more than 2%. In addition, the GRI-Mech 3.0 showed the best prediction of NO emission in comparison with the experimental data.

As reviewed above, a lot of numerical studies on fuel-rich combustion for syngas production in porous media burner have been conducted applying different detailed mechanisms, the influence of these kinetics on prediction of premixed combustion for fuel-lean combustion in porous burner has been revealed. However, it is still not certain the influence of the prediction of syngas production for fuel-rich combustion in porous media using different chemical reaction mechanisms. To save computation time, one may prefer to use a smaller detailed kinetic for modeling of syngas production in porous burner, but it was not known if this mechanism have the same accurate in predicting the combustion characteristics as the more detailed mechanisms. At the same time, one-dimensional model was widely used to save computational time and the two-dimensional study is scarce, which is more accurate to compute the heat loss to the surrounding through burner walls.

The aim of the present work is to investigate the influence of chemical reaction mechanisms on predictions of the temperature profiles, chemical structures and therefore the output of the syngas production in the exhaust gas, using a two-temperature two-dimensional model. In contrast to previous studies which emphasized on the effect of chemical kinetics on fuel-lean combustion in porous media, we explore the syngas production for fuel-rich combustion in porous media.

## PHYSICAL MODEL

A two-layer porous burner reported by Zeng et al. (2017) is considered in the present work to study the sensitive of different kinetics to the predictions of syngas production in porous media. As shown in **Figure 1**, the burner was designed to study the effect of CO<sub>2</sub> addition on the conversion efficiency of CH<sub>4</sub> partial combustion within packed bed, which consists of two layers of alumina pellets with different diameters. In the upstream section the burner was filled with 2–3 mm alumina pellets that are 20 mm long, while the downstream layer was filled with 7.5 mm alumina pellets with length of 60 mm. The premixed mixture of methane with different amount of CO<sub>2</sub> and air was feed into the burner and combustion waves were restricted near the interface of the upstream and downstream sections. For simplification, the pellet diameter in the upstream section is assumed to be a constant value of 2.5 mm. 2-D computations are considered in this work to save computational time. To simplify the problem, the following assumptions are made;

- (1) The alumina pellets are assumed to be inert homogeneous and optically thick media, the solid radiation is taken

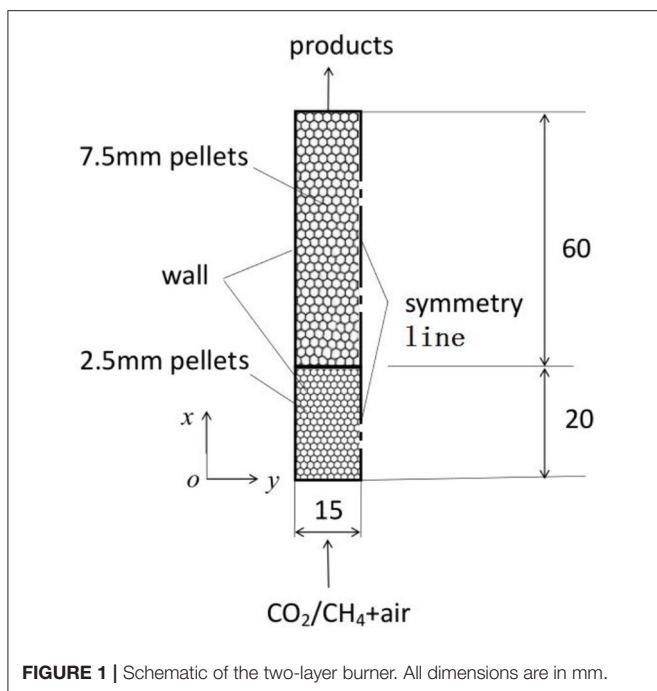


FIGURE 1 | Schematic of the two-layer burner. All dimensions are in mm.

into account using the effective radiation thermal conductivity model.

- (2) Gas flow in the packed bed is assumed to be laminar and gas radiation is ignored.
- (3) The porosity variation near the tube wall is ignored and the thermal conductivity of the packed bed is the same for the two layers.

The chemistry is treated with two detailed kinetics and a reduced chemical mechanism in the computation. These mechanisms include two full mechanisms compiled by the Gas Research Institute, namely GRI-Mech 1.2 (32 species, 177 reactions), GRI-Mech 3.0 (53 species, 325 reactions), and DRM 19 (Kazakov and Frenklach, 1994) (20 species, 58 reactions) which is a reduced mechanism based on GRI-Mech 1.2. The gas thermal and transport properties are obtained from the Chemkin and Tranit packages (Kee et al., 1986).

Under the above assumptions, a set of differential equations can be obtained.

Continuity equation:

$$\nabla \cdot (\rho_g \mathbf{v}) = 0 \quad (1)$$

where  $\rho_g$  represents the gas density;  $\mathbf{v}$  denotes the velocity vector.

Vertical momentum equation

$$\nabla(\rho_g \mathbf{v} u) = \nabla(\mu \nabla u) - \frac{\Delta p}{\Delta x} \quad (2)$$

Where  $u$  represents the vertical velocity;  $\mu$  is dynamic viscosity,  $p$  is the pressure.

Horizontal momentum equation:

$$\nabla(\rho_g \mathbf{v} v) = \nabla(\mu \nabla v) \quad (3)$$

where  $v$  denotes the horizontal velocity. The pressure loss in the vertical direction is computed as (Ergun, 1952),

$$\frac{\Delta p}{\Delta x} = 150 \frac{(1 - \varepsilon)^2}{\varepsilon^3} \frac{\mu u'}{d^2} + 1.75 \frac{1 - \varepsilon}{\varepsilon^3} \frac{\rho_g u'^2}{d} \quad (4)$$

where  $\varepsilon$  is the porosity of the porous media,  $d$  is the pellet diameter,  $u'$  is superficial velocity and  $u' = \varepsilon u$ .

Gas phase energy equation:

$$\nabla \cdot (\rho_g c_g \mathbf{v} T_g) = \nabla \cdot (\lambda_g \nabla T_g) + h_v (T_s - T_g) + \sum_i \omega_i h_i W_i \quad (5)$$

where  $T_g, \lambda_g, c_g$  are the gas temperature, thermal conductivity and specific heat, respectively.  $T_s$  denotes the solid temperature;  $\omega_i, W_i$  are the chemical reaction rate and molecular weight of species  $i$ .  $h_v$  is the volumetric convective heat-transfer coefficient between the gas and solid phases (Kaviany, 1994),

$$h_v = 6 \varepsilon \text{Nu}_v \lambda_g / d^2, \text{Nu}_v = 2 + 1.1 \text{Pr}^{1/3} \text{Re}^{0.6} \quad (6)$$

where  $\text{Nu}_v, \text{Pr}$ , and  $\text{Re}$  is the Nusslet number, Prandtl number, and Reynolds number, respectively.

Solid phase energy equation:

$$\nabla \cdot (\lambda_{\text{eff}} \nabla T_s) + h_v (T_g - T_s) = 0 \quad (7)$$

Where  $\lambda_{\text{eff}}$  is the effective thermal conductivity of the porous media and can be expressed as  $\lambda_{\text{eff}} = \lambda_s + \lambda_{\text{rad}}$ ,  $\lambda_s$ , and  $\lambda_{\text{rad}}$  are the solid thermal conductivity. We assume that the thermal conductivities for the two sections are same and the influence needs to be further studied. The radiative heat transfer coefficient of the alumina pellets, respectively.  $\lambda_{\text{rad}}$  is expressed as (Serguei et al., 1996).

$$\lambda_{\text{rad}} = (32 \varepsilon \sigma d / 9(1 - \varepsilon)) T_s^3 \quad (8)$$

Species conservation equation:

$$\nabla \cdot (\rho_g \mathbf{v} Y_i) - \nabla \cdot (\rho_g \nabla Y_i) - \omega_i W_i = 0 \quad (9)$$

Where  $Y_i$  is mass fraction of species  $i$ .

## BOUNDARY CONDITIONS

The following boundary conditions are specified in the model:

1) Inlet

$$\begin{aligned} T_g = T_s = 300 \text{ K}, u = u_0, v = 0 \\ Y_{\text{CH}_4} = Y_{\text{CH}_4, \text{in}}, Y_{\text{O}_2} = Y_{\text{O}_2, \text{in}}, Y_{\text{CO}_2} = Y_{\text{CO}_2, \text{in}}, \\ Y_{\text{N}_2} = Y_{\text{N}_2, \text{in}} \end{aligned} \quad (10)$$

2) Outlet

$$\frac{\partial T_g}{\partial x} = \frac{\partial T_s}{\partial x} = \frac{\partial (Y_i)}{\partial x} = 0. \quad (11)$$

3) Solid temperature at the inlet and outlet;

$$\lambda_{\text{eff}} \frac{\partial T_s}{\partial x} = -\varepsilon_r \sigma (T_{s,\text{in/out}}^4 - T_0^4) \quad (12)$$

$\varepsilon_r$  is the solid surface emissivity,  $\sigma$  is the Stefan-Boltzmann constant,  $T_0$  is ambient temperature.

4) At  $y = 15$  mm, symmetry conditions are imposed;

$$\frac{\partial T_g}{\partial y} = \frac{\partial T_s}{\partial y} = \frac{\partial Y_i}{\partial y} = \frac{\partial u}{\partial y} = v = 0 \quad (13)$$

5) Wall

At  $y = 0$  mm, heat loss to the surroundings through the burner walls by convective heat transfer is considered and heat flux  $\dot{q}$  is defined as,

$$\dot{q} = \frac{\lambda}{\delta} (T_{\text{wall}} - T_0) \quad (14)$$

where  $\lambda$  is thermal conductivity of insulation,  $\delta$  is thickness of insulation.

## INITIAL CONDITIONS AND SOLUTION

The governing equations presented above are numerically solved by a CFD software Fluent 15.0. To allow the gas and solid phases have different temperatures, user defined function and scalars provided by Fluent 15.0 are used to solve a separate energy equation for the solid phase. Radiative and conductive transport through the packed bed, convective heat transfer between the gas and solid phases is taken into account in the model, as shown in the above Equation (7).

The SIMPLE algorithm is used to handle the pressure and velocity coupling. At the downstream, the solid temperature with a thickness of 4 mm is set to be 1,800 K to model the ignition process. Mesh independence of the results are verified. The computational domain is discretized into 600 cells in the upstream section and 3,600 cells in the downstream section. When the solution is converged, the mesh of the reaction zone is densified.

A residual error of  $10^{-6}$  for energy equations and  $10^{-3}$  for all other equations are taken as convergence criteria.

The syngas energy conversion efficiency is defined as:

$$\eta_{e-s} = \frac{Y_{\text{H}_2} \times \text{LHV}_{\text{H}_2} + Y_{\text{CO}} \times \text{LHV}_{\text{CO}}}{Y_{\text{CH}_4,\text{in}} \times \text{LHV}_{\text{CH}_4}} \quad (15)$$

where  $\text{LHV}_{\text{H}_2}$ ,  $\text{LHV}_{\text{CO}}$ ,  $\text{LHV}_{\text{CH}_4}$  are the low heating value of  $\text{H}_2$ ,  $\text{CO}$ , and  $\text{CH}_4$ , respectively. **Table 1** presents the symbol used in this work.

## RESULTS AND DISCUSSION

### Temperature Distributions

In the experiment (Zeng et al., 2017) the equivalence ratio and air flow rate are fixed while the ratio ( $\alpha$ ) between the  $\text{CO}_2$  and  $\text{CH}_4$  is changed from 0 to 1. The solid thermal conductivity of

alumina is  $7.22 \text{ W/m} \cdot \text{K}$  at  $T = 1,000 \text{ K}$ , according to reference by Munro (1997). For volume average method used in this work, the thermal conductivity of packed bed is defined as 0.04 times of the solid thermal conductivity at  $T = 1,000 \text{ K}$  as reference, this means that thermal conductivity of the packed bed is  $0.2888 \text{ W/m} \cdot \text{K}$  unless otherwise stated. **Table 2** shows the simulation cases carried out in this work. In the computation, for all computed cases the equivalence ratio is set to be a fixed value of 1.5 and the thermal conductivity of packed bed is varied due to uncertainty of its values. In the following, the temperature reported is along the centerline of the burner.

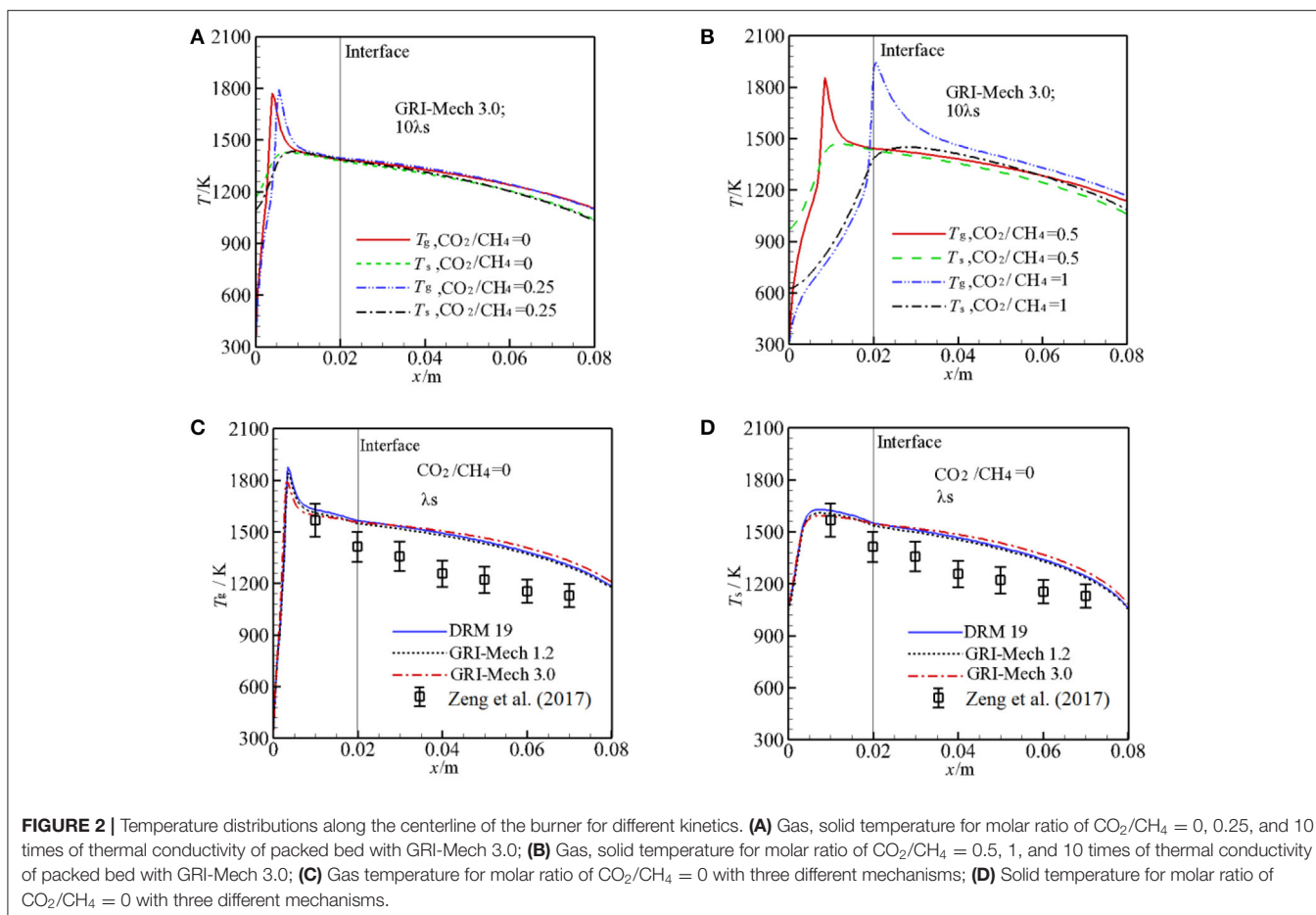
**Figure 2** illustrates the predicted  $T_g$  and  $T_s$  at the centerline ( $y = 0$  mm) for different  $\alpha$  as well as experimental values for comparison. **Figures 2A,B** shows predicted  $T_g$ ,  $T_s$  with GRI-Mech 3.0 at  $\lambda_s = 2.888 \text{ W/m} \cdot \text{K}$ . The calculated results show that the flame shifts from upstream of burner to the interface of two sections as  $\alpha$  is increased from 0 to 1. One may expect that the maximum combustion temperature decreases with  $\alpha$  due to injection of greater amount of  $\text{CO}_2$  to the burner, but the opposite trend is observed as shown in **Figures 2A,B**. One of the reasons for this phenomenon is due to the different flame stabilization positions where  $h_v$  are different.  $h_v$  is getting greater as the pellet diameter is decreased, as shown in Equation (6). At the reaction zone, the reaction heat is redistributed through convective heat

**TABLE 1** | Symbols used in this work.

Nomenclature	
$d$ diameter of spheres, m	$h_i$ the molar enthalpy of species $i$ , KJ/Kg
$h_v$ convective heat transfer between the solid and gas phases, $\text{W/m}^3 \text{ K}$	$\rho$ pressure, Pa
$T$ temperature, K	$T_0$ ambient temperature, K
$u$ vertical velocity, m/s	$v$ horizontal velocity, m/s
$W_i$ molecular weight of species $i$ , $\text{Kg/Kmol}$	$x$ vertical coordinate, m
$X$ molar fraction	$y$ horizontal coordinate, m
$Y$ mass fraction	
Greek symbols	
$\varphi$ equivalent ratio	$\lambda$ thermal conductivity, $\text{W/m K}$
$\lambda_{\text{eff}}$ effective thermal conductivity, $\text{W/m K}$	$\lambda_{\text{rad}}$ radiation conductivity, $\text{W/m K}$
$\rho$ density, $\text{Kg/m}^3$	$\varepsilon$ porosity
$\omega_i$ reaction rate of species $i$ , $\text{Kg/Kmol}$	$\sigma$ Stefan-Boltzmann constant, $\text{W/m}^2 \text{ K}^4$
$\alpha$ volume flow ratio between $\text{CO}_2$ and $\text{CH}_4$	$\delta$ Thickness of insulation, m
$\mu$ dynamic viscosity, $\text{Pa}_s$	$\eta_{e-s}$ syngas energy conversion efficiency
$\varepsilon_r$ solid surface emissivity	
subscripts	
g gas	s solid

**TABLE 2** | Simulation cases carried out in this work.

Equivalence ratio	1.5
The ratio of $\text{CO}_2/\text{CH}_4$ and its corresponding inlet velocity (m/s)	0 (0.1365), 0.25 (0.1412), 0.5 (0.1458), 1 (0.1551)

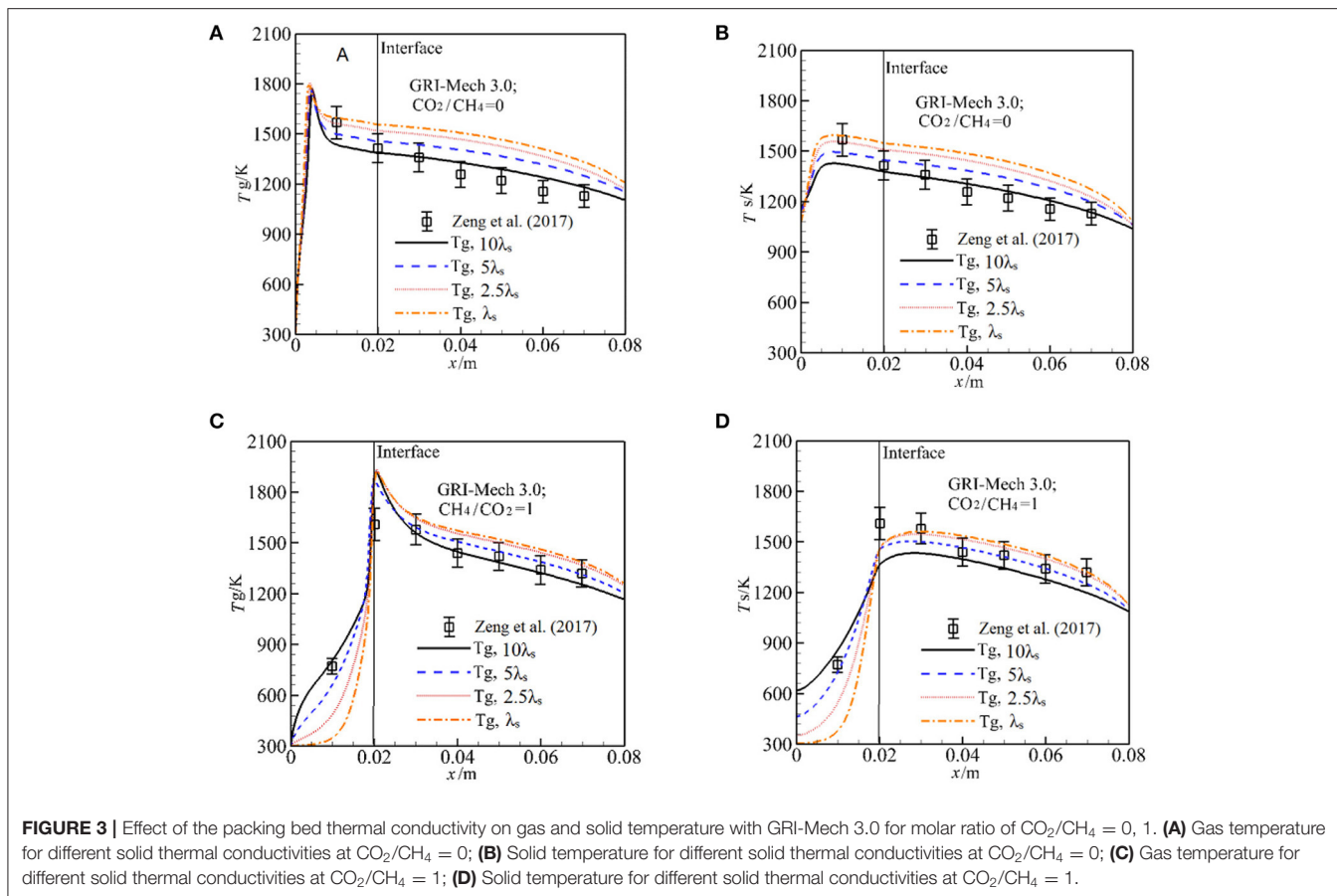


transfer between the two phases. When the flame is stabilized near the interface, the convective heat transfer weakens and thus the temperature difference between the two phases is enlarged, which results to higher gas combustion temperature in the reaction zone for the smaller pellet diameter.

**Figures 2C,D** show the predicted  $T_g$ ,  $T_s$  by three different kinetics for  $\alpha = 0$  at  $\lambda_s = 0.2888 \text{ W/m}\cdot\text{K}$  as well as experiment results (Zeng et al., 2017) for comparison. For  $\alpha = 0$ , it can be seen that the predicted  $T_g$ ,  $T_s$  are similar through the burner for the different three kinetics and the temperature differences predicted by the three kinetics are quiet small except for the reaction zone. In the pre-heat zone, the predicted  $T_g$  is almost independent of the mechanisms used. Small difference is observed downstream the reaction zone. The more detailed mechanism is used, the greater peak temperature is obtained in the computation as shown in **Figure 2C**. In the reaction zone the combustion temperature by the DRM 19 is highest and reaches up to 1,879 K,  $T_g$  by GRI-Mech 3.0 is lowest and the value is 1,786 K. In a word, the temperature distributions in the pre-heat and post reaction zone are almost independent of the mechanisms used, in the reaction zone the peak temperature predicted by different kinetics is rather small. Considering the computation cost and time, choosing a smaller mechanism for predicting temperature

distribution in the burner may be a good choice and rather accuracy can be obtained, when the detailed components of the syngas is not taken into consideration. It is noted that the predicted  $T_g$  and  $T_s$  by the three kinetics are always greater than the corresponding experiment values, in the following this deviation will be discussed.

In the experimental study of Zeng et al. (2017),  $\lambda_s$  was not presented and the effect of  $\lambda_s$  on the syngas production was not clear. We test the sensitive of  $\lambda_s$  to  $T_g$  and  $T_s$  by increasing  $\lambda_s$  by 10 times with other parameters are fixed. The results with GRI-Mech 3.0 for  $\alpha = 0$  are shown in **Figures 3A,B**. One can see that  $\lambda_s$  has significant influence on the temperature distribution in the burner. For  $\alpha = 0$ , the flame is stabilized near the burner inlet. The temperatures both for gas and solid phases in the entire burner decrease with  $\lambda_s$ . This is because an increase in  $\lambda_s$  leads to enhance heat condition in the solid phase, more heat is conducted through the solid phase, thus the temperature gradient is getting lower with  $\lambda_s$ . According to the Equation (12), the heat loss to the surrounding through burner inlet and outlet is increased as  $\lambda_s$  is increased, which leads to decrease in temperature in the burner. The predictions with 10  $\lambda_s$  match well with experimental results and the predictions are greater than the experimental value as  $\lambda_s$  is decreased.



For  $\alpha = 1$ , as shown in **Figures 3C,D**, the flame stabilizes just downstream the interface,  $T_s$  distribution in the pre-heat zone is opposite to that for  $\alpha = 0$ ,  $T_s$  is increased with  $\lambda_s$ . This is attributed to the fact that the heat recirculation from the high solid temperature zone to the downstream direction is enlarged when  $\lambda_s$  is increased, which leads to increase in  $T_s$  in the first section of the burner, thus the gas mixture is effectively preheated and  $T_g$  is increased.

## Chemical Structure

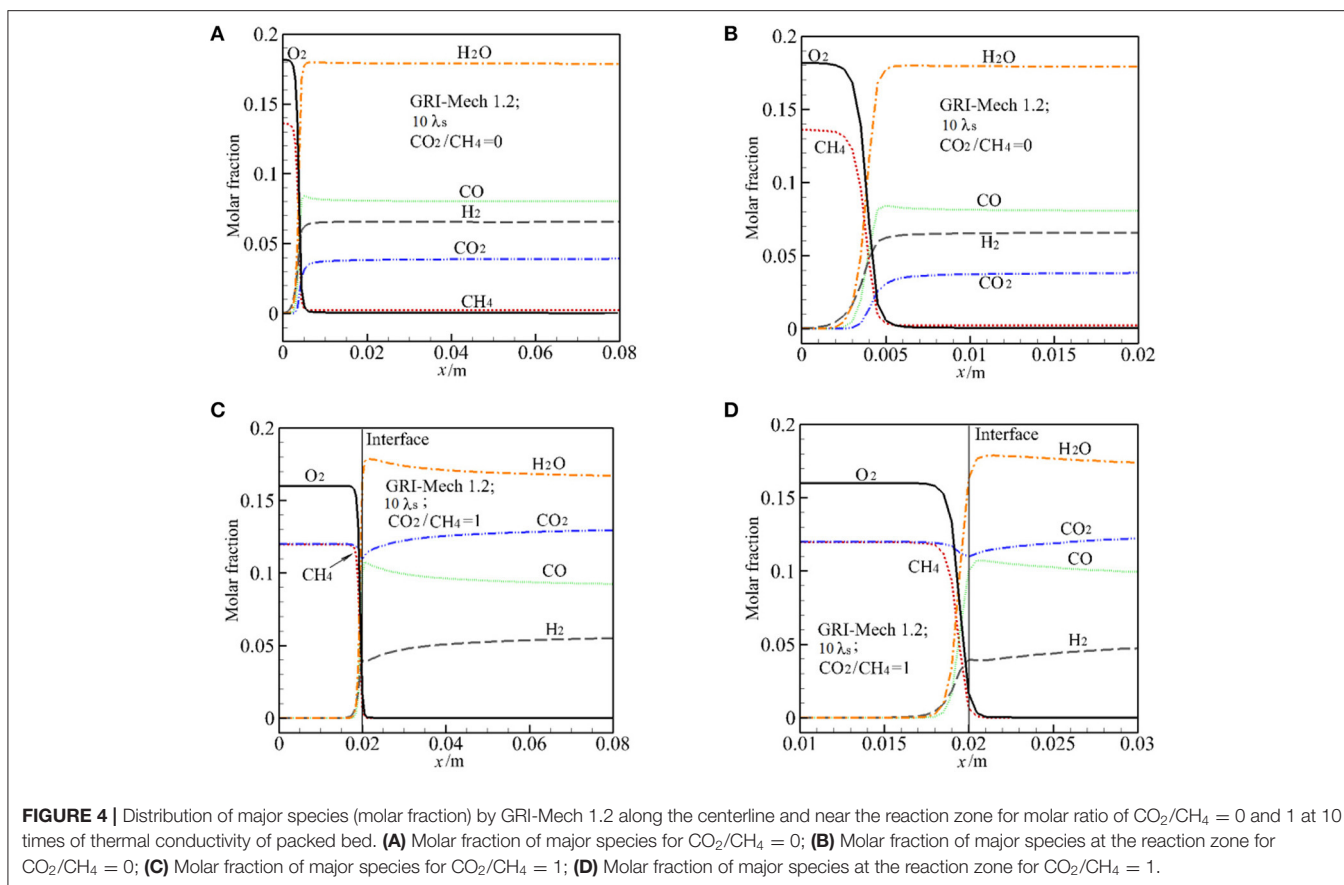
The major species in the exhaust gases includes  $\text{H}_2$ ,  $\text{H}_2\text{O}$ ,  $\text{CO}$ ,  $\text{CO}_2$ , and  $\text{CH}_4$ . Consistent with the experiment (Zeng et al., 2017), the **Figure 4** show the predicted species based on the wet base. **Figure 4** presents the predictions of molar fraction of  $\text{H}_2\text{O}$ ,  $\text{O}_2$ ,  $\text{H}_2$ ,  $\text{CO}_2$ ,  $\text{CO}$ ,  $\text{CH}_4$  by GRI-Mech 1.2 along the vertical direction for  $\alpha = 0, 1$  at  $10\lambda_s$ . For visible, the major species near the reaction zone is also presented in the **Figure 4**. According to Futko (2003), the combustion wave is composed of the preheating zone, an exothermic zone with partial combustion of methane in the reaction  $\text{CH}_4 + 0.5\text{O}_2 = \text{CO} + 2\text{H}_2$  (16), and an endothermic zone characterized by the reforming processes  $\text{CO} + \text{H}_2\text{O} = \text{CO}_2 + \text{H}_2$  (17),  $\text{CH}_4 + \text{H}_2\text{O} = \text{CO} + 3\text{H}_2$  (18). For  $\alpha = 0$ , it can be seen that extensive reaction occurs in a small region with length about 3 mm near the burner inlet.

Methane begins to break down near the burner inlet,  $\text{CH}_4$  and  $\text{O}_2$  are quickly consumed in the exothermic zone. As shown in **Figures 4A,B**, all the syngas components almost peak after the exothermic zone in this case, only small change in major species is observed due to the reforming reaction. This indicates that the reaction (18) and (19) contribute little to the  $\text{CO}$  and  $\text{H}_2$  production in the endothermic zone in this case.

For  $\alpha = 1$ , the predicted distribution of major species is similar to that of  $\alpha = 0$ , except for the distribution of  $\text{CO}_2$  in the exothermic zone. In this zone  $X_{\text{H}_2}$  and  $X_{\text{CO}}$  increase sharply and then  $X_{\text{H}_2}$  increases slowly while  $X_{\text{CO}}$  reduces slightly in the endothermic zone. As shown in **Figures 4C,D**,  $X_{\text{CO}_2}$  decreases first in the reaction zone, this means that  $\text{CO}_2$  reacts and is consumed. Then  $X_{\text{CO}_2}$  continually increases along the vertical direction. It can be seen from **Figures 4A,B** that, after the exothermic zone the variation rate of the major species for  $\alpha = 1$  is greater than that for  $\alpha = 0$ . This is the effect of  $\text{CO}_2$  injection in the burner and also the effect of reforming reaction (17) and (18).

## Major Species in the Exhaust Gases and Conversion Efficiency

**Figure 5** depicts the predicted major species of  $\text{H}_2$ ,  $\text{CO}$ ,  $\text{CO}_2$ ,  $\text{CH}_4$  in the exhaust gases as a function of  $\alpha$  for three different



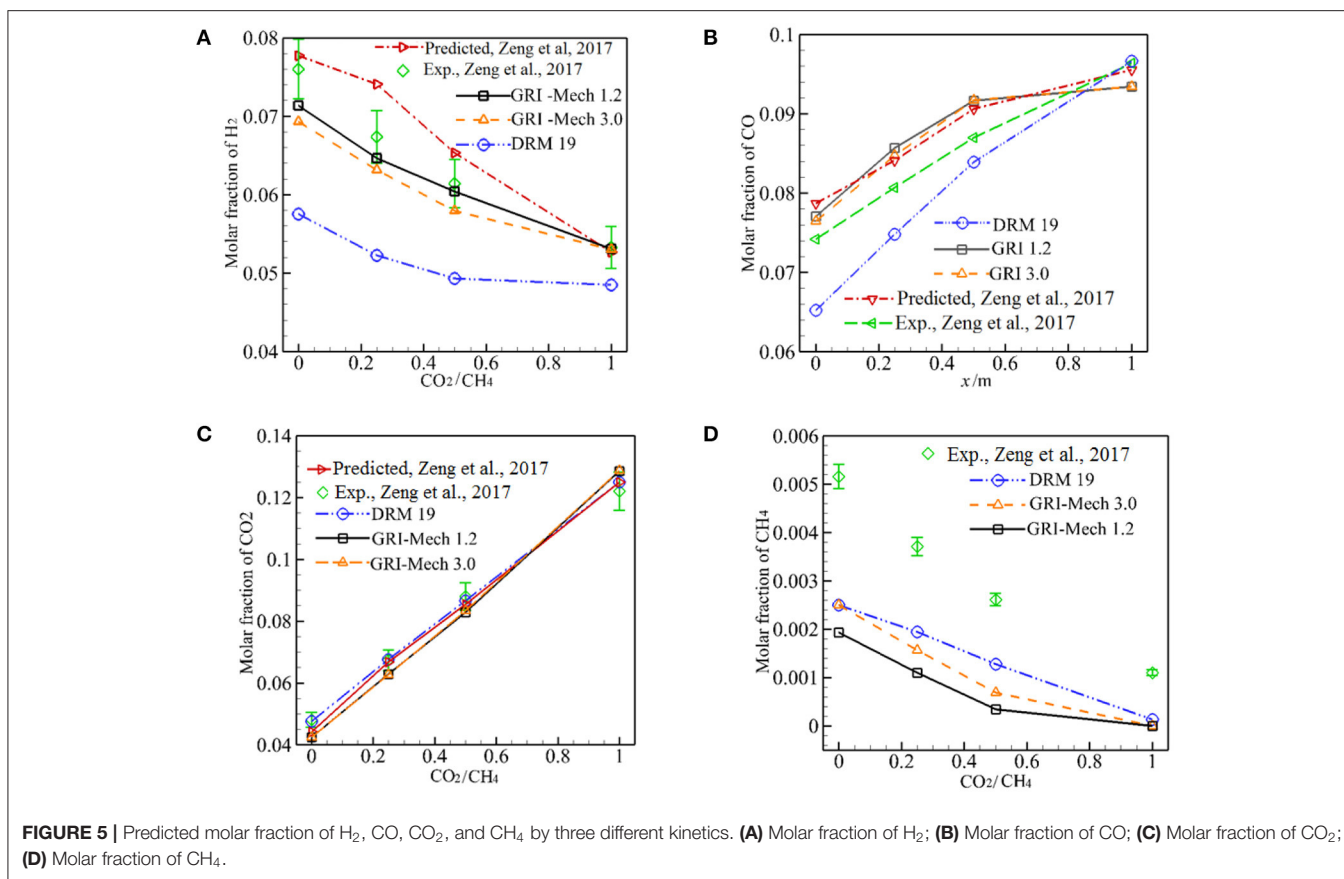
kinetics at  $\lambda_s = 0.2888 \text{ W/m}\cdot\text{K}$ . In **Figure 5** the experimental and computational results with Peters by Zeng et al. (2017) are also shown for comparison. As shown in **Figure 5A**, both the experimental results and predictions show that  $X_{\text{H}_2}$  decreases with increasing  $\alpha$  from 0 to 1 and the predicted  $X_{\text{H}_2}$  by three different kinetics are lower than the experimental values, whereas the computational results by Zeng et al. (2017) are greater than the experimental values. The predicted values by GRI-Mech 1.2 and GRI-Mech 3.0 match well with the experiment when the measurement error is taken into account. The prediction by DRM 19 also shows the same trend with experiment, but its values are significantly lower than the experimental values. For  $\alpha = 1$ , the calculated results by GRI-Mech and Peters precisely predict the experimental results, this may be due to the dilution effect of the  $\text{CO}_2$  in the fuel.

**Figure 5B** shows the comparison of predicted  $Y_{\text{CO}}$  with experimental results and Zeng et al. (2017) for three different kinetics. The predictions by GRI-Mech 1.2 and GRI-Mech 3.0 are greater than the corresponding experimental results, as shown in **Figure 5B**. Qualitative agreement between the numerical and experimental results can be noted when the measurement error is taken into consideration. It is noted that the predictions by DRM19 deviates significantly from experimental results.

As demonstrated in **Figures 5A–C**,  $X_{\text{CO}}$  increases while  $X_{\text{H}_2}$  decreases with  $\alpha$ . Meantime,  $X_{\text{CO}_2}$  increases with  $\alpha$ , although part of the  $\text{CO}_2$  reacts and is consumed in the exothermic zone as reactant when  $\text{CO}_2$  was injected into the burner. The reaction (17) is an important reformation reaction in the endothermic zone and the injection of  $\text{CO}_2$  into the burner may promote the inverse reaction (17), this may be responsible for the continue increase in  $X_{\text{CO}}$  and decrease in  $X_{\text{H}_2}$  when  $\alpha$  is increased from 0 to 1.

**Figures 5C,D** presents predictions of  $X_{\text{CO}_2}$ ,  $X_{\text{CH}_4}$  by GRI-Mech, DRM19, and Peters (Zeng et al., 2017). All the combustion models precisely predict  $X_{\text{CO}_2}$  for  $0 \leq \alpha \leq 1$ . Although all combustion models predict the trend of  $X_{\text{CH}_4}$  with  $\alpha$ , but the predictions are about two times of the corresponding experimental values.

To test the effect of  $\lambda_s$  on conversion efficiency,  $\lambda_s$  is varied from  $0.2888 \text{ W/m}\cdot\text{K}$  to  $2.888 \text{ W/m}\cdot\text{K}$  and the computation is conducted with GRI-Mech 3.0. These results are presented in **Figure 6**. As discussed above, a lower  $\lambda_s$  serves to reduce heat conduction through the solid phase and it is advantageous to form a high solid temperature zone around the reaction zone, thus results in a higher combustion temperature. The increased temperature drives the chemical kinetic to yield a higher percentage conversion. As shown in **Figure 6A**,  $X_{\text{H}_2}$



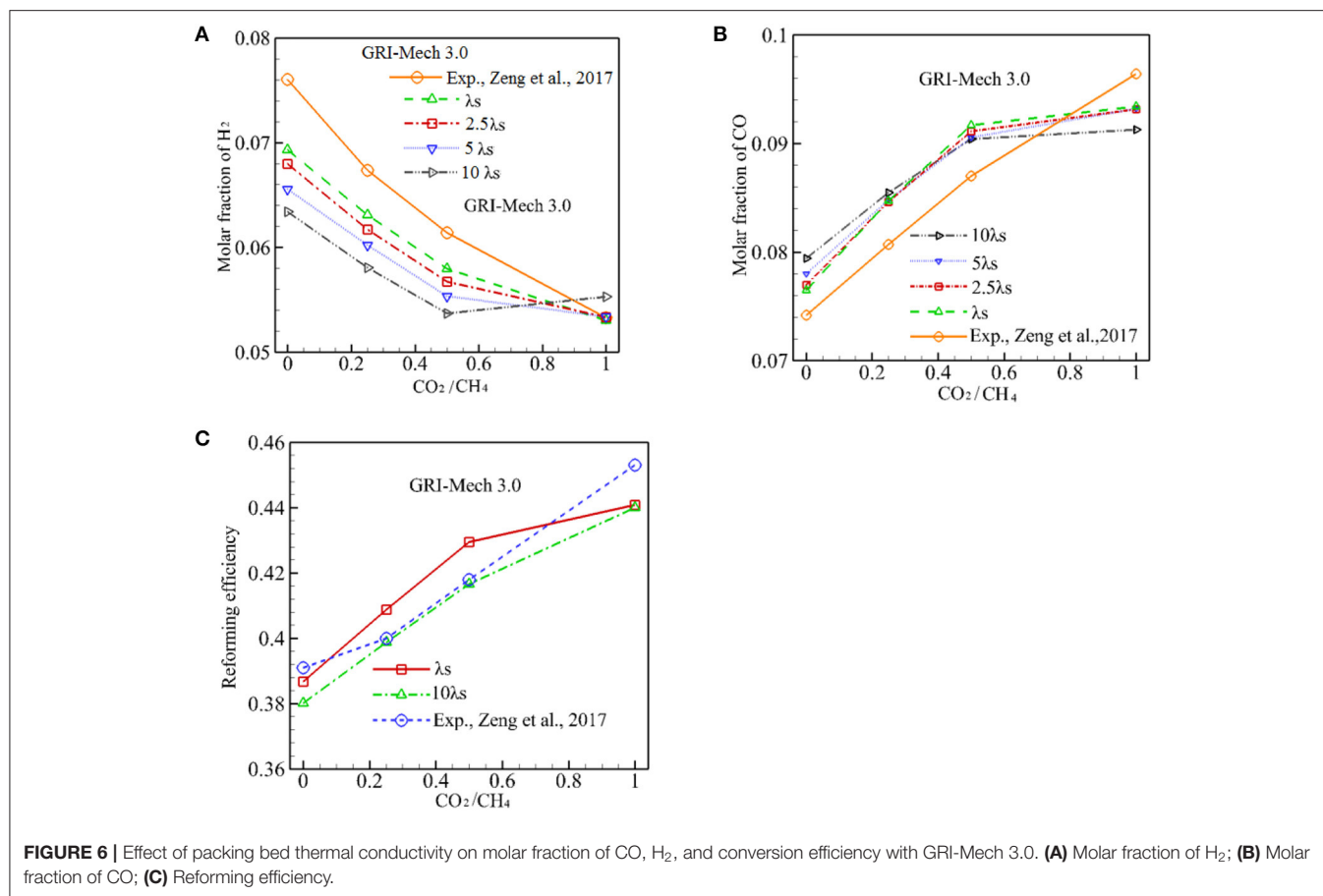
always increases when  $\lambda_s$  is reduced for  $\alpha \leq 0.5$ . However, the effect of  $\lambda_s$  on the production of H<sub>2</sub> diminishes for  $\alpha = 1$ . The effect of  $\lambda_s$  on the production of CO is shown in **Figure 6B**, in which it can be seen that increasing in  $\lambda_s$  results in a small increase in  $X_{CO}$  for  $\alpha \leq 0.25$ . Then the opposite trend is observed for  $\alpha > 0.25$ ,  $X_{CO}$  decreases with  $\alpha$ . A combined effect of on the syngas production is shown in **Figure 6C**, one can see that a decrease in  $\lambda_s$  results in a very small increase in the percentage conversion. For example, the conversion efficiency increases from 41.66 to 42.95% as  $\lambda_s$  is decreased from 2.888 to 0.2888 W/m·K for  $\alpha = 0.5$ , thus the increase in conversion efficiency can be ignored.

## CONCLUSIONS

The influence of chemical mechanisms on the syngas production for rich CO<sub>2</sub>/CH<sub>4</sub> and air mixture combustion in a two-layer porous burner is investigated using a two-dimensional two-temperature model with GRI-Mech 1.2, GRI-Mech 3.0 and a reduced mechanism (DRM19) based on GRI 1.2. In the computation, the equivalence ratio is a fixed value of 1.5 while the ratio of CO<sub>2</sub> to CH<sub>4</sub> is changed from 0 to 1. The sensitive of predicted temperature distributions in the burner and major

species in the exhaust gases to the mechanisms used in the model is conducted. The major conclusions from the present study are as follows;

- (1) Kinetic has no obvious influence on the temperature profiles in the burner expect for the narrow exothermic zone. The predicted temperature distributions by the three kinetics match well with experimental results. For predictions of temperature profiles without consideration of major species, using DRM 19 is recommended to save computational time.
- (2) The predicted major species (H<sub>2</sub>, CO, CO<sub>2</sub>) by GRI-Mech 1.2 and GRI-Mech 3.0 indicates that the two mechanisms have almost the same accuracy in predicting detailed components, little difference is observed for the whole investigated range. Thus, when the NO<sub>x</sub> emission is not focus of the study, GRI-Mech 1.2 is recommended to save computational time. However, the predicted molar fraction of H<sub>2</sub> and CO by DRM 19 is under-predicted compared to experimental values. The three kinetics over-predicted the molar fraction of CH<sub>4</sub> by a factor about two times of the experimental values.
- (3) Thermal conductivity of the porous media used in the burner has significant effect on predicting the syngas productions. Increase in the thermal conductivity leads to a decrease



in the combustion temperature, and thus increases in H<sub>2</sub> and decreases in CO, a very small increase in conversion efficiency is observed when the thermal conductivity is decreased by a factor of 10 times and this effect can be ignored.

## DATA AVAILABILITY STATEMENT

All datasets generated for this study are included in the article/supplementary material.

## REFERENCES

- Araya, R., Araus, K., Utria, K., and Toledo, M. (2014). Optimization of hydrogen production by filtration combustion of natural gas by water addition. *Int. J. Hydr. Energy* 39, 7338–7345. doi: 10.1016/j.ijhydene.2014.02.113
- Bowman, C. T., Hanson, R. K., Davidson, D. F., Gardiner, W. C., Lissianski, J. V., Smith, G. P., et al. (2009). Available online at: <https://me.berkeley.edu>
- Dhamrat, R. S., and Ellzey, J. L. (2006). Numerical and experimental study of the conversion of methane to hydrogen in a porous media reactor. *Combust. Flame* 144, 698–709. doi: 10.1016/j.combustflame.2005.08.038
- Dobrego, K. V., Gnesdilov, N. N., Lee, S. H., and Choi, H. K. (2008). Overall chemical kinetics model for partial oxidation of methane in inert porous media. *Chem. Eng. J.* 144, 79–87. doi: 10.1016/j.cej.2008.05.027

## AUTHOR CONTRIBUTIONS

JS, MM, and HL conceived and designed the study. YoL analyzed the data. YaL and YD wrote the manuscript.

## FUNDING

The authors wish to acknowledge the support to this work by the National Natural Science Foundation of China (Nos. 51876107) and SDUT & Zibo City Integration Development Project of China (Grant No. 2018ZBXC084).

- Dorofeenko, S. O., and Polianczyk, E. V. (2016). Conversion of hydrocarbon gases to synthesis gas in a reversed-flow filtration combustion reactor. *Chem. Eng. J.* 292, 183–189. doi: 10.1016/j.cej.2016.02.013
- Drayton, M. K., Saveliev, A. V., Kennedy, L. A., Fridman, A. A., and Li, Y. E. (1998). Syngas production using superadiabatic combustion of ultra-rich methane-air mixtures. *Symp. Combust.* 27, 1361–1367. doi: 10.1016/S0082-0784(98)80541-9
- Ergun, S. (1952). Fluid flow through packed columns. *Chem. Eng. Prog.* 48, 89–94.
- Fan, A. W., Li, L. H., Yang, W., and Yuan, Z. L. (2019). Comparison of combustion efficiency between micro combustors with single- and double-layered walls: a numerical study. *Chem. Eng. Process.* 137, 39–47. doi: 10.1016/j.cep.2019.02.004
- Fan, A. W., Zhang, H., and Wan, J. (2017). Numerical investigation on flame blow-off limit of a novel microscale Swiss-roll combustor with a bluff-body. *Energy* 123, 252–259. doi: 10.1016/j.energy.2017.02.003

- Futko, S. I. (2003). Kinetic analysis of the chemical structure of waves of filtration combustion of gases in fuel-rich compositions. *Combust. Explos. Shock Waves* 39, 437–447. doi: 10.1023/A:1024786805591
- Gonzalez, H., Caro, S., Toledo, M., and Olguin, H. (2018). Syngas production from polyethylene and biogas in porous media combustion. *Int. J. Hydr. Energy* 43, 4294–4304. doi: 10.1016/j.ijhydene.2018.01.050
- Hsu, P. F., and Matthews, R. D. (1993). The necessity of using detailed kinetics in models for premixed combustion within porous media. *Combust. Flame* 93, 457–466. doi: 10.1016/0010-2180(93)90145-S
- Kaviany, M. (1994). *Principles of Convective Heat Transfer*. New York, NY: Springer-Verlag.
- Kazakov, A., and Frenklach, M. (1994). Available online at: <http://combustion.berkeley.edu/gri-mech/>
- Kee, R. J., Dixon, G. L., Warnatz, J., Coltrin, M. E., and Miller, J. A. (1986). *A Fortran Computer Code Package for the Evaluation of Gas Phase Multi-Component Transport Properties*. Report SAND86-8246, Sandia National Laboratories.
- Kennedy, L. A., Bingue, J. P., Saveliev, A. V., and Foutko, S. I. (2000). Chemical structures of methane-air filtration combustion waves for fuel-lean and fuel-rich conditions. *Proc. Combust. Inst.* 28, 1431–1438. doi: 10.1016/S0082-0784(00)80359-8
- Kennedy, L. A., Saveliev, A. V., and Fridman, A. A. (1999). *Proceedings of the Mediterranean Combust. Naples: Symposium*, 105–139.
- Kostenko, S. S., Ivanova, A. N., Karnaukh, A. A., and Polianczyk, E. V. (2014). Simulation of the methane conversion by partial oxidation in a porous medium reactor. *Chem. Eng. J.* 238, 100–110. doi: 10.1016/j.cej.2013.09.012
- Liu, H., Dong, S., Li, B. W., and Chen, H. G. (2009). Parametric investigations of premixed methane-air combustion in two-section porous media by numerical simulation. *Fuel* 89, 1736–1742. doi: 10.1016/j.fuel.2009.06.001
- Mauss, F., and Peters, N. (1993). “Reduced kinetic mechanisms for premixed methane-air flames,” *Reduced Kinetic Mechanisms for Application in Combustion Systems*, eds N. Peters and B. Rogg (Berlin: Springer), 58–75. doi: 10.1007/978-3-540-47543-9\_5
- Mohammadi, I., and Hossainpour, S. (2013). The effects of chemical kinetics and wall temperature on performance of porous media burners. *Heat Mass Transfer* 49, 869–877. doi: 10.1007/s00231-013-1126-y
- Mujeebu, A. M. (2016). Hydrogen and syngas production by superadiabatic combustion -a review. *Appl. Energy* 173, 210–224. doi: 10.1016/j.apenergy.2016.04.018
- Munro, M. (1997). Evaluated material properties for a sintered alpha-alumina[J]. *J. Am. Ceram. Soc.* 80, 1919–1928. doi: 10.1111/j.1151-2916.1997.tb03074.x
- Serguei, I. F., Stanislav, I. S., and Serguei, A. Z. (1996). Superadiabatic combustion wave in a diluted methane-air mixture under filtration in a packed bed. *Sym. Combust.* 26, 3377–3382. doi: 10.1016/s0082-0784(96)80186-x
- Toledo, M., Bubnovich, V., Saveliev, A., and Kennedy, L. (2009). Hydrogen production in ultrarich combustion of hydrocarbon fuels in porous media. *Int. J. Hydr. Energy* 34, 1818–1827. doi: 10.1016/j.ijhydene.2008.12.001
- Toledo, M., Gracia, F., Caro, S., Gomez, J., and Jovicic, V. (2016). Hydrocarbons conversion to syngas in inert porous media combustion. *Int. J. Hydr. Energy* 41, 5857–5864. doi: 10.1016/j.ijhydene.2016.02.065
- Trimis, D., and Durst, F. (1996). Combustion in a porous media-advances and applications. *Combust. Sci. Technol.* 121, 153–168. doi: 10.1080/00102209608935592
- Wang, S. X., Yuan, Z., I., and Fan, A. W. (2019). Experimental investigation on non-premixed CH<sub>4</sub>/air combustion in a novel miniature Swiss-roll combustor, chemical engineering and processing- process *Intensification*. 139, 44–50. doi: 10.1016/j.cep.2019.03.019
- Wang, Y. Q., Zeng, H. Y., Shi, Y. X., and Cai, N. S. (2018). Methane partial oxidation in a two-layer porous media burner with Al<sub>2</sub>O<sub>3</sub> pellets of different diameters. *Fuel* 217, 45–50. doi: 10.1016/j.fuel.2017.12.088
- Xu, Y., Dai, Z., Li, C., Li, X., Zhou, Z., Yu, G., et al. (2014). Numerical simulation of natural gas noncatalytic partial oxidation reformer. *Int. J. Hydr. Energy* 39, 9149–9157. doi: 10.1016/j.ijhydene.2014.03.204
- Zeng, H. Y., Wang, Y. Q., Shi, Y. X., Ni, M., and Cai, N. S. (2017). Syngas production from CO<sub>2</sub>/CH<sub>4</sub> rich combustion in a porous media burner: experimental characterization and elementary reaction model. *Fuel* 199, 413–419. doi: 10.1016/j.fuel.2017.03.003
- Zheng, C., Cheng, L., Bingue, J. P., Saveliev, A., and Cen, K. (2012a). Partial oxidation of methane in porous reactor: part I. unidirectional flow. *Energy Fuels* 26:47Z. doi: 10.1021/ef300851z
- Zheng, C., Cheng, L., Cen, K., Bingue, J. P., and Saveliev, A. (2012b). Partial oxidation of methane in a reciprocal flow porous burner with an external heat source. *Int. J. Hydr. Energy* 37, 4119–4126. doi: 10.1016/j.ijhydene.2011.11.142

**Conflict of Interest:** The authors declare that the research was conducted in the absence of any commercial or financial relationships that could be construed as a potential conflict of interest.

Copyright © 2020 Shi, Mao, Li, Liu, Liu and Deng. This is an open-access article distributed under the terms of the Creative Commons Attribution License (CC BY). The use, distribution or reproduction in other forums is permitted, provided the original author(s) and the copyright owner(s) are credited and that the original publication in this journal is cited, in accordance with accepted academic practice. No use, distribution or reproduction is permitted which does not comply with these terms.